

Article

Not peer-reviewed version

Atmospheric CO₂: A 2-Box model accurately tracks ¹⁴C and ¹³C spanning 200 years and estimates global uptake of fossil fuel emissions

[Stephen E. Taylor](#)*

Posted Date: 25 October 2023

doi: 10.20944/preprints202310.1593.v1

Keywords: Anthropogenic Emissions; Revelle Factor; Exchange Flux; Bomb Pulse



Preprints.org is a free multidiscipline platform providing preprint service that is dedicated to making early versions of research outputs permanently available and citable. Preprints posted at Preprints.org appear in Web of Science, Crossref, Google Scholar, Scilit, Europe PMC.

Copyright: This is an open access article distributed under the Creative Commons Attribution License which permits unrestricted use, distribution, and reproduction in any medium, provided the original work is properly cited.

Article

Atmospheric CO₂: A 2-Box Model Accurately Tracks ¹⁴C and ¹³C Spanning 200 Years and Estimates Global Uptake of Fossil Fuel Emissions

S E Taylor

Geomatix Ltd, UK; set@geomatix.net

Abstract: Based upon a radically new approach, this paper describes a 2-box absolute flow model that calculates the CO₂ transfer between the atmosphere and a terrestrial / ocean mixing reservoir. Given the inputs of anthropogenic fossil fuel emissions (CO₂ff), atmospheric CO₂ mixing-ratio and nuclear weapons bomb yields, the model calculates atmospheric $\delta^{13}\text{C}$ and $\Delta^{14}\text{C}$ time-series, with the level of agreement for $\delta^{13}\text{C}$ being to within $\pm 0.05\%$, for $\Delta^{14}\text{C}$ to within $\pm 3\%$, spanning 200 years. The model contains only seven internal parameters which are varied to optimize the fit. Yet according to conventional wisdom this model should not work. It is commonly held that the ¹³C and ¹⁴C isotopic forms of carbon bypass seawater carbonate chemistry, resulting in very different absorption properties (Revelle factor) as compared to ¹²C. This study rejects this assumption, and uses the same residence time and reservoir mixing properties for all isotopes. The paper includes an analysis justifying why the isotopic bypass of the Revelle factor is not significant. The study describes the use of the model to track CO₂ff takeup using two separate measures, a) the amount of molecular CO₂ff remaining in the atmosphere and b) the amount of atmospheric growth attributable to CO₂ff, thereby resolving discrepancies in published values.

Keywords: Anthropogenic Emissions; Revelle Factor; Exchange Flux; Bomb Pulse

1. Introduction

Unlike nett values of CO₂ exchange flux between the atmosphere and the land/ocean, the absolute each-way values are not accurately known, yet they are key to understanding the carbon cycle and to estimating the effects of anthropogenic CO₂ fossil fuel emissions, (CO₂ff) (IPCC (Ed.) 2013; IPCC(Ed) 2021). The exchange flow is caused by diurnal and seasonal variations which, as the earth spins on its axis and orbits the sun, alternately cause absorption and emission, arising from cyclical diurnal and seasonal changes in seawater solubility, photosynthesis, plant decay and respiration. This complicated pattern of both positive and negative fluxes implies that while absorption is occurring at one geographical location, there is simultaneous emission at another. This two-way exchange flow is estimated at approximately 210GtC in each direction per year, easily exceeding the one way CO₂ff despite its rise from 2.5 GtC in 1960 to 9 GtC in 2021 (Friedlingstein et al., 2022). However, although CO₂ff is smaller than exchange flow, it is still significant when compared to the imbalance in the exchange flux. In the 1970s box models were developed (e.g. Oeschger et al., 1975) to describe the carbon cycle; however, their popularity waned as General Circulation Models (GCMs) became common which, although requiring greater computer resources, could create gridded global maps of the carbon-related processes.

Symbol Table and Acronyms

A, A _{abs} , A _s	Relative, absolute standard, and specific ¹⁴ C activity
A ₁₄ [], R ₁₄ []	¹⁴ C/C ratio: Atmosphere, Reservoir
AF	Airborne Fraction
A _{FF} [],	Atmospheric Fossil Fuel content
A _{FL} [], A _{NL} []	Atmospheric Fossil Level, Natural (non-fossil) Level (0-1)
B	Listed Annual Bomb Yield (MegaTonnes)
C	Atmospheric carbon mass GtC

CO _{2ff}	Anthropogenic fossil fuel CO ₂ emissions
F ¹⁴ C	¹⁴ C Carbon Flux
F _a , F _e , F _i	Atmospheric CO ₂ flux: Anthropogenic, exiting, going in
GCM	General Circulation Models
GtC	Gigatonnes Carbon: equals 10 ⁹ tonnes of carbon
IPCC	Intergovernmental Panel on Climate Change
k _e	Atmospheric CO ₂ Exchange rate
M _T , M _i	Mass of Mixture and Mass of portion i
R, R ¹⁴	Isotopic ratio, ¹⁴ C/C ratio
RCO₂	Relative Reservoir Size
R _T , R _i	Ratio of a specific molecule in mixture, T and portion i
Y_b	Bomb Yield in megatons
α_t	Removal time (years)
β	Rel. proportion of CO_{2ff} mixing into atmosphere
Δ ¹⁴ C	An offset age & fractionation corrected ratio of ¹⁴ C/C †
Δ¹⁴C_{init}	Initial value of Δ¹⁴C at start of iteration
ΔC	Change in C at each iteration
ΔT	Change in time at each iteration
⊙	Isotopic ratio relative to a standard
⊙ ¹³ C	An offset measure of ¹³ C/C ratio relative to a standard
⊙ ¹³ C _F , ⊙ ¹³ C _N	⊙ ¹³ C: For Fossil CO ₂ , Natural (non-fossil CO ₂)
⊙¹³C_{init}, ⊙¹³C_{ff}	The value of ⊙¹³C : Initial, fossil fuels
⊙ ¹³ C _M , ⊙ ¹³ C _W	⊙ ¹³ C for a Measurement, for Wood
⊙ ¹⁴ C	An offset measure of ¹⁴ C/C ratio relative to a standard
⊙ _⊙ ⊙ _⊙ ⊙ ₁ , ⊙ ₂	Standard deviation of fit of time series: Total, 1, 2
(t)	Denotes a function value at time, t
[i]	Denotes the value at each iteration, i

Bold-shaded indicates the seven internal optimized parameters; † ¹⁴C/¹²C ratio rel. to hypothetical value of atmospheric ¹⁴C in 1950 (See Stuiver & Polach, 1977).

Undoubtedly GCMs have a significant role to play in modeling the complexity of the global carbon cycle. However, there are advantages in adopting a strategy of top-down simplification using box models, rather than adopting the open-ended system of micro-accounting in the GCMs. This is because simpler models by their very nature are "better testable" (Popper, 1934) and are more likely to shed light on errors in formulation, focusing on the most significant factors. This paper describes a 2-box model that derives ¹⁴C and ¹³C isotopic ratios given anthropogenic emissions and CO₂ mixing ratio. The major differences between this and previous box models are; a) its use of atmospheric CO₂ level as an input, not an output, and b) its use of absolute gross flow, not net flow. This model accurately calculates isotopic ¹⁴CO₂ and ¹³CO₂ time-series spanning some 200 years (including the bomb pulse). Yet according to conventional wisdom the model should not work. It is widely known that the carbonate ions form a buffer solution limiting the absorption rate of CO₂, this effect being known as the Revelle factor. It is commonly held that the ¹³C and ¹⁴C isotopic forms of carbon bypass seawater carbonate chemistry, exhibiting very different absorption properties as compared to ¹²C. (Tans 1993, Joos 1994, Harvey 2000), although this was never proven. This study demonstrates this assumption is invalid, since it uses the same residence time and reservoir mixing properties for all isotopes and yet produces accurate results. For a full discussion see section 7.1.

1.1. Radiocarbon

The global isotopic abundance of ¹³C and ¹⁴C present within atmospheric CO₂ is accurately known, having been measured in samples from tree rings (Stuiver & Quay 1981), ice cores (Rubino et al., 2013), and the atmosphere (Stuiver et al., 1998; D6). While ¹³C is radioactively stable and forms around one percent of atmospheric carbon, ¹⁴C undergoes radioactive decay with a half-life of 5700 ±

30 years (Kutschera 2013), comprising about 1 part in 10^{12} . There is virtually no presence of ^{14}C in fossil fuel since it has all radioactively decayed. The $^{14}\text{C}/^{12}\text{C}$ ratio decreased between 1800 and 1960 because of the lack of ^{14}C in fossil fuel emissions. Then in 1960 atmospheric nuclear weapons testing caused a sudden doubling of the absolute level, also known as ^{14}C activity. Since 1975 it has decreased (D6), partially due to washout from the exchange flow which contains a somewhat lower level of ^{14}C but also because of dilution arising from fossil fuels CO_2 input, which is ^{14}C depleted (Levin, 2010). This process is known as "Suess" dilution (Suess 1955). Turning now to ^{13}C , its presence in fossil fuels is reduced when compared with the atmosphere, but only by around 2% (Stuiver and Polach, 1977); this small reduction arising from fractionation, i.e. because the larger less mobile isotopic CO_2 molecules are less likely to become embedded in leaves and fossil carbon. Measurements show that the atmospheric $^{13}\text{C}/^{12}\text{C}$ ratio has decreased during the past 200-year period (D4), due to dilution by fossil fuel carbon which contains the lower level of ^{13}C and washout from the exchange flow. (see Discussion)

2. CO_2 Absolute Flow Finite Reservoir Model

The model describes the movement of CO_2 and its carbon isotopes between atmosphere and terrestrial / oceanic mixing reservoir. See Figure 1. The size of this mixing reservoir is an "effective" value, corresponding to the combined effect of the ocean and terrestrial storage. The idea of effective values is commonplace in many fields of engineering, science and economics. Economic inflation represents, in a single figure, the average of many different price increases on many items. Productivity measures the effective value created by each hour of work. Effective resistance in electronic engineering or hydraulics gives the overall resistance of a complex system to current or fluid flow. The assumption in each of these examples is that a single value can account for some property which is distributed throughout a complex system. The elegance of this method is its ability, unlike other methods, to determine the effective values without requiring a detailed audit of the underlying constituent components.

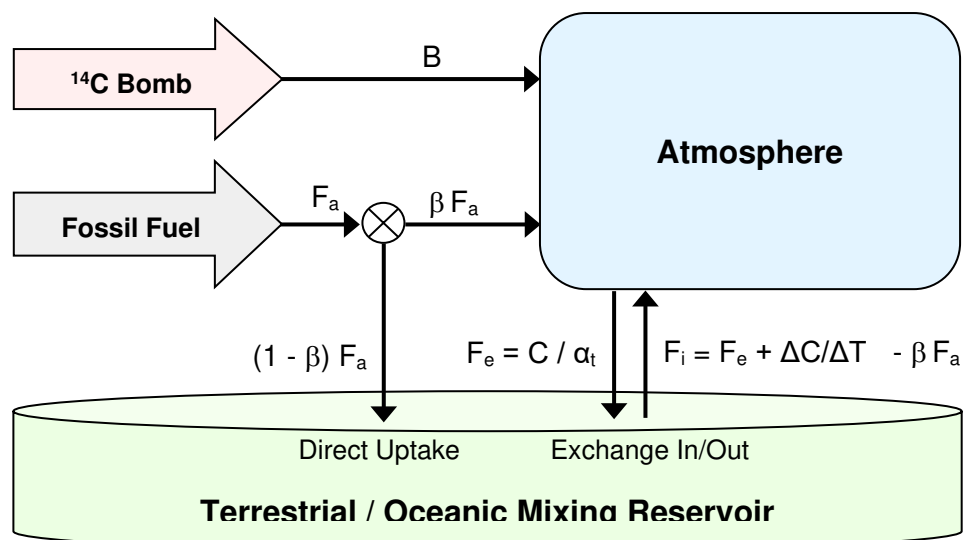


Figure 1. CO_2 Finite Reservoir Two-Box Model. The model describes the CO_2 flux between the reservoir and atmosphere, including its isotopic carbon contents. Isotopic mixing occurs in the two storage regions, atmosphere and reservoir. A proportion, β of anthropogenic fossil fuel CO_2 , F_a , enters the atmosphere, while the remainder, $1 - \beta$ enters the reservoir by direct uptake. At each iteration, the CO_2 flux outflow F_e is proportional to atmospheric CO_2 , $C(t)$; its isotopic content corresponding to that of the atmosphere. The CO_2 flux in, F_i is determined from F_e and the rate of change $\Delta C / \Delta T$, with its isotopic content corresponding to that of the reservoir, R . Atomic weapons ^{14}C $B(t)$ directly enters the atmosphere at intervals and amounts determined by historical records of atmospheric atomic weapons testing and bomb yield.

The two boxes in the model are considered well-mixed. At each iteration, the new isotopic concentration within the reservoir and atmosphere caused by the incoming ^{13}C and ^{14}C is calculated. We now explain the ideas behind the model's formulation. Using a similar manner and notation as Tans et al.,(1993) and Cawley (2011) we have

$$dC/dT = F_a + F_i - F_e$$

where C is the atmospheric carbon mass, F_a is the anthropogenic flux, F_i is the flux in and F_e is the flux exiting the atmosphere. Many authors e.g. Oeschger (1975), assume a pre-industrial equilibrium but their method is not suitable for our purposes since it relies on the calculation of a net flux; it is essential that F_i and F_e are kept separate because we will need the separate fluxes to calculate the isotopic flows. We first need an expression which connects the atmospheric CO_2 mass C , to the outflow, F_e an obvious choice being

$$F_e = k_e C \quad (1)$$

Absolute inflow, as opposed to outflow, can then be calculated by balancing the budget; if the atmosphere is growing by an amount ΔC in time ΔT it must be receiving the outflow plus the growth amount minus the inflow from anthropogenic input, which is anthropogenic output, F_a , times the proportion which arrives in the atmosphere, β , hence we obtain

$$F_i = F_e + \Delta C / \Delta T - \beta F_a \quad (2)$$

Equation (1) satisfies the obvious requirement that the exit flux F_e , is zero when CO_2 mass C is zero. A further requirement, satisfied by equation(2) is that when $F_i - F_e$ is zero the atmospheric growth $\Delta C/\Delta T$, equals the anthropogenic input, F_a . These requirements distinguish this absolute flow description from other descriptions such as provided by Oeschger (1975) and Cawley (2011). This formulation leads to a radically different solution from conventional box models. It avoids the necessity to include allowance for seawater carbonate chemistry, because the outflow behaviour is lumped into a single constant, k_e which is empirically derived. Similarly the inflow behaviour, being calculated by balancing the budget, eliminates the need to provide a bottom-up audit of CO_2 release from the ocean or land due to outgassing, respiration, decay and combustion. Once outflow is derived, inflow can be defined from the known anthropogenic input and CO_2 measurements. We assume the constant k_e applies equally to the calculation of outflow for all three carbon species $^{14}\text{CO}_2$, $^{13}\text{CO}_2$ and $^{12}\text{CO}_2$ (see Discussion).

The model estimates the nuclear bomb yield of ^{14}C each year, $B_{14}[i]$, by using a bomb yield multiplication factor, Y_b , this being one of the seven optimisation parameters. The bomb yield in megatons was obtained from records of atomic weapons atmospheric test detonations [D5] and was converted using Y_b . A simple time delay of one year was used to allow for atmospheric mixing. The initial values i.e. $\delta^{13}\text{C}_{\text{init}}$, $\Delta^{14}\text{C}_{\text{init}}$, are parameters within the model and determine the initial level of the curves in Figures 3 & 4, while $\delta^{13}\text{C}_{\text{FF}}$ determine the curve slopes in Figures 4 & 5.

2.1. Mass-Balance and Isotopic Dilution

If a number of gases are mixed but do not react, and each component gas, i , has a mass M_i , then from the law of conservation of mass (also known as Mass Balance)

$$M_T = \sum M_i$$

If within each component gas there is a specific molecule present in a ratio to its mass, R_i , then, since that specific molecule is conserved, the resulting mixture (e.g. paint mixing) having mass M_T has a ratio R_T given by

$$R_T = \sum R_i M_i / M_T \quad (3)$$

Equation (3) applies to the situation of mixing of isotopic gases. For practical reasons associated with historical measurements of radioactivity, studies of isotopic mixtures normally utilize the ratio of the sample activity, A_s to a standard sample activity A_{abs} , this ratio being known as the relative

specific activity, A . Its value is then offset by one to provide the radioactivity scale, δ written (see Strenstrom 2011) in the form

$$\delta = (A_s/A_{abs}) - 1 = A - 1 \quad (4)$$

In this scale, although δ increases linearly with A_s , its value is offset to be zero at the value of the absolute standard (often chosen to approximate background level), as for example in the cases of $\delta^{13}C$ and $\delta^{14}C$. Applying (4) and substituting A_{s_i} for each component R_i of the mixture, leads after some algebraic manipulation, to

$$\delta_T = \Sigma (\delta_i M_i) / M_T \quad (5)$$

The similarity with Eq.(3) shows that although δ is defined by an offset ratio scale we can still directly apply equation(3) to calculate the resulting value of δ_T for the mixture. The above scheme forms the basis for the system of equations $A_{14}[i]$, $R_{14}[i]$, $A_{FF}[i]$ and $R_{FF}[i]$ shown in the implementation section below.

2.2. Fractionation

The model generates values of $\delta^{14}C$ but comparison is required with measured values of $\Delta^{14}C$, which incorporates a fractionation correction to "translate the measured activity to the activity the sample would have had if it had been wood" (Strenstrom 2011). The correction formulae, a function of $\delta^{13}C$, may be derived from equations by Strenstrom 2011 using equations 25, 28, 38, or Stuiver & Polach 1977 p356, 360, Table 1, where A_{SN} is the normalised specific sample activity, A_s is the specific activity of the atmosphere or reservoir, A_{abs} is the absolute specific standard, $\delta^{13}C_M$ is the ^{13}C sample measurement, and $\delta^{13}C_W$ is the ^{13}C standard for wood, giving

$$\delta^{14}C = A_s / A_{abs} - 1$$

$$\Delta^{14}C = A_{SN} / A_{abs} - 1$$

$$A_{SN} = A_s [(1 + \delta^{13}C_W) / (1 + \delta^{13}C_M)]^2$$

Eliminating A_s , A_{abs} and A_{SN} gives

$$\Delta^{14}C = [1 + \delta^{14}C] [(1 + \delta^{13}C_W) / (1 + \delta^{13}C_M)]^2 - 1$$

The fractionation correction was applied to $\delta^{14}C$, with $\delta^{13}C$ for wood as -25‰ (the standard), and $\delta^{13}C_M$ being taken from the model. The correction is quite small, $\Delta^{14}C$ is around 10‰ less than $\delta^{14}C$ at the peak of the bomb pulse ($\delta^{14}C \sim 800$ ‰) decreasing to 0.03‰ ($\delta^{14}C \sim 0$).

2.3. Age Correction

The ^{14}C half-life of 5700 ± 30 years (Kutschera, W., 2013), which translates to a radioactive decay of around 2% over the period from 1820 to 2020. However, we know the steady production of stratospheric ^{14}C roughly balances the amount of ^{14}C decay since the two are in approximate equilibrium. Therefore neither ^{14}C decay nor natural stratospheric ^{14}C production were included in the model.

2.4. Implementation

The implementation processes several calculations at each iteration. The following 3 equations are based upon. The amount of CO_2 in the atmosphere is C , its removal time is α_t , the atmosphere outflow is F_e , the inflow is F_i , and the amount of CO_2 initially in the reservoir is R , with the square brackets '[i]' referring to the value at iteration i , hence the iteration relationships (using equations 1 and 2) become:-

$$F_e[i] = C[i] / \alpha_t$$

$$F_i[i] = F_e[i] + C[i] - C[i-1] - \beta F_a[i-1]$$

$$R[i] = R[i-1] + F_e[i] - F_i[i] + (1 - \beta) F_a[i-1]$$

The ratio of $^{14}\text{C} / \text{C}$ in the atmosphere is denoted by A_{14} and for the reservoir by R_{14} . The new amount is given by the previous amount added to the input amounts with the output amount being subtracted, all divided by the total mass, see equation 5. If necessary we include the annual ^{14}C production due to atomic weapons bomb input, B_{14} . Hence

$$A_{14}[i] = (A_{14}[i-1] \cdot C[i-1] + F_i[i-1] \cdot R_{14}[i-1] - F_e[i-1] \cdot A_{14}[i-1] + B_{14}[i-1]) / C[i]$$

$$R_{14}[i] = (R_{14}[i-1] \cdot R[i-1] - F_i[i-1] \cdot R_{14}[i-1] + F_e[i-1] \cdot A_{14}[i-1]) / R[i]$$

Similarly, the relative atmospheric and reservoir fossil fuel content A_{FF} and R_{FF} , are calculated on a scale of 0 to 1 using the values at the previous iteration levels, where A refers to the atmosphere, and R the reservoir and subscripts FL means fossil fuel level, and NL means natural non-fossil level,

$$A_{FF}[i] = (A_{FF}[i-1] \cdot C[i-1] + F_i[i-1] \cdot R_{FF}[i-1] - F_e[i-1] \cdot A_{FF}[i-1] + \beta F_a[i-1]) / C[i]$$

$$R_{FF}[i] = (R_{FF}[i-1] \cdot R[i-1] - F_i[i-1] \cdot R_{FF}[i-1] + F_e[i-1] \cdot A_{FF}[i-1] + (1 - \beta) F_a[i-1]) / R[i]$$

$$A_{FL}[i] = C[i] \cdot A_{FF}[i], \quad A_{NL}[i] = C[i] - A_{FL}[i]$$

$$R_{FL}[i] = R_{FF}[i] \cdot R[i], \quad R_{NL}[i] = R[i] - R_{FL}[i]$$

The offset isotopic ratiometric measure for ^{13}C is $\delta^{13}\text{C}$ and that for ^{14}C is $\Delta^{14}\text{C}$. These are calculated from the iterative series by:-

$$\delta^{13}\text{C} = \delta^{13}\text{C}_{FF} \cdot A_{FF} + \delta^{13}\text{C}_N (1 - A_{FF}), \quad \Delta^{14}\text{C} = (A_{14} - 1)$$

Initial Conditions: $F_i[0] = F_e[0]$, $A_{14}[0] = 1$, $R_{14}[0] = 1$, $A_{FF}[0] = 0$, $R_{FF}[0] = 0$

In accounting for isotopic concentration, it is not necessary to explicitly embed an attenuation factor as discussed by Stuiver & Quay (1981), or to account separately for Suess dilution (1955) because they are implicitly represented.

3. Method

The input data was selected between 1750 to 2020 from the appropriate data source listing [D1-D6] and entered into a spreadsheet. The cell formulae were set to correspond to those iteration equations given in the Appendix. The solution was found by minimizing the discrepancy between observed and calculated values of $\delta^{13}\text{C}$ and $\Delta^{14}\text{C}$ using the standard "Solver" function of Microsoft Excel. The solver system was set to use the 7 parameters shown in Table 1 using the default solver options. For version details see appendix.

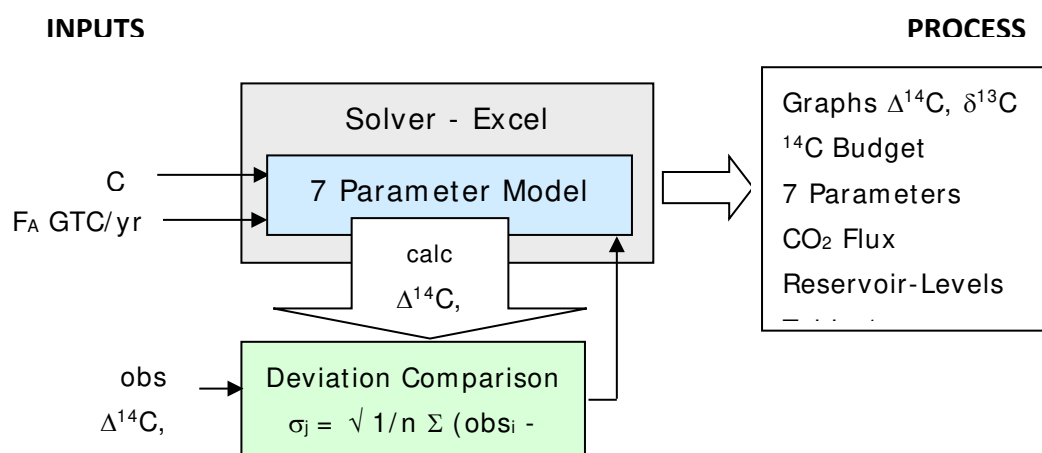


Figure 2. Solution Optimisation. The 7 parameter model and the deviation comparison formulae are implemented as cell formulae within Microsoft Excel. The deviation comparison formulae compares the measured time-series values of atmospheric $\Delta^{14}\text{C}$ and $\delta^{13}\text{C}$ with the calculated values. The Add-In Solver was used to numerically minimise the standard deviation by varying the values of the 7 parameters, providing the above outputs shown below in this study.

The optimisation-solution process is shown in fig. 2 above. The standard deviations σ_1 and σ_2 between observed and predicted was determined for $\delta^{13}\text{C}$ and $\Delta^{14}\text{C}$. The square root of this product gives the overall geometric mean standard deviation, σ . Hence

$$\sigma_j = \sqrt{1/n \otimes (\text{obs}_i - \text{calc}_i)^2} \quad (3)$$

$$\sigma_{\otimes} = (\sigma_1 \times \sigma_2)^{1/2} \quad (4)$$

The Excel Solver was set to minimise the value of the target cell containing the overall geometric mean standard deviation by variation of the seven parameters shown in Table 1. Only one true constant was used, atmospheric capacity, which was taken to have a value of 2.124 ppm GtC-1 as published by Ballantyne (2012). Thus the model uses a very different technique from standard modeling techniques for deriving anthropogenic and non-anthropogenic flux. It optimises the seven parameters to fit $\delta^{13}\text{C}$ and $\Delta^{14}\text{C}$ ratios, and the flux and mixing reservoir levels emerge as by-products from this process.

4. Results

The results divide into three main types; the optimised seven parameters themselves, the graphical output, and flux tables. Flux and cumulative flux are model outputs.

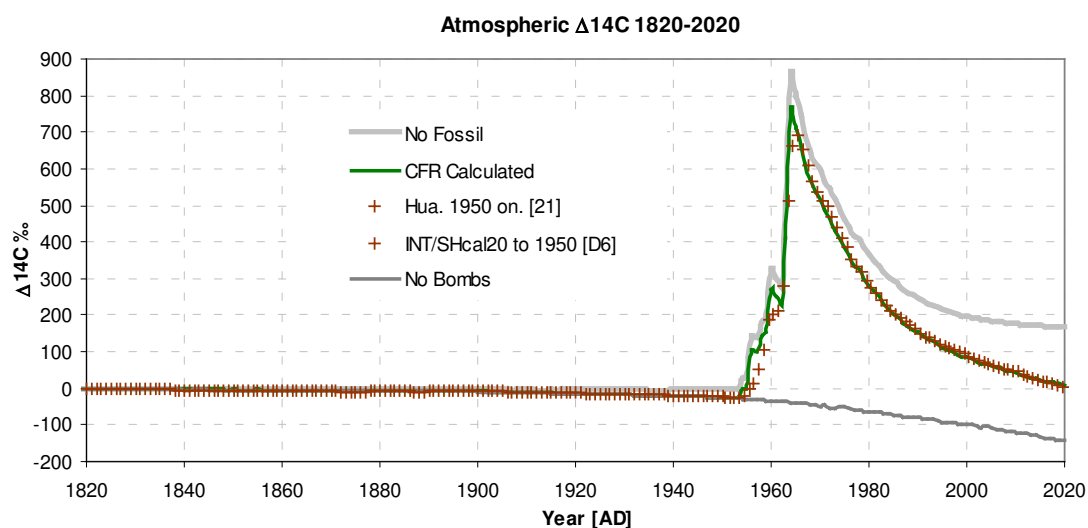


Figure 3. Atmospheric $\Delta^{14}\text{C}$ 1820-2020. showing 130 values before 1950 [D6] and 70 values from 1968 onwards (Hua et al., 2022). Standard deviation of observed and predicted is $\sigma = 3.0\text{‰}$, excluding values during the rising pulse from 1950 to 1968. For "no bombs" and "no fossil". See text.

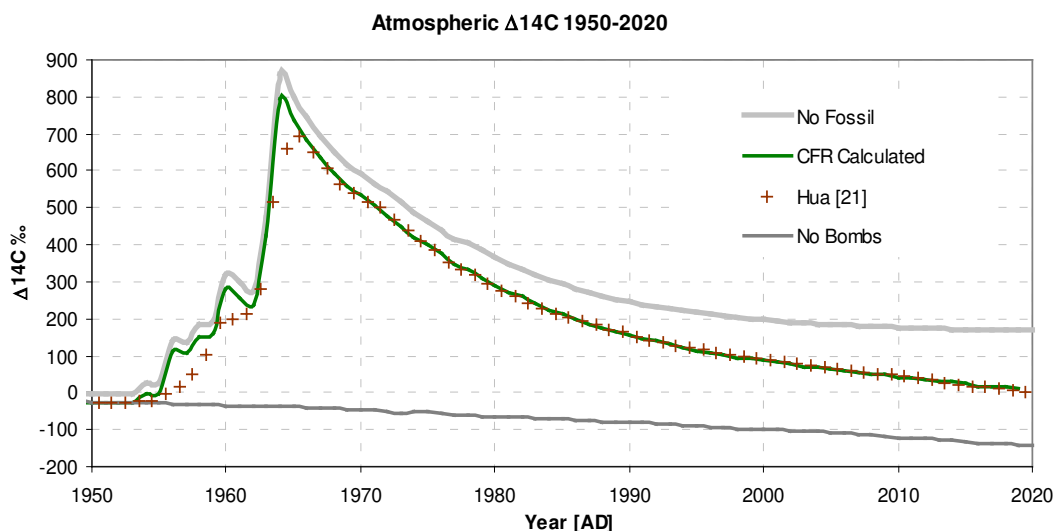


Figure 4. Atmospheric $\Delta^{14}\text{C}$ between 1950 and 2020 showing the "bomb pulse" to 2020. For "no bombs" and "no fossil" see text.

Figures 3 & 4 show actual and modelled values of $\Delta^{14}\text{C}$. In total 340 observed data points were used giving a total overall standard deviation of 0.39‰. The quality of fit is excellent, with a standard deviation of 3‰. In figure 3 the slight decrease from 1820 to 1940 is due to Suess dilution, the magnitude of the dilution being somewhat reduced by reservoir inflow, giving excellent agreement with observations. Figure 4 shows the bomb pulse plotted as $\Delta^{14}\text{C}$. Initially the pulse shape is a decaying exponential but then, as it is influenced by Suess dilution and the re-emergence of ^{14}C from the mixing reservoir, becomes more of a linear fall. Nevertheless, despite these complicating factors, the predicted and observed values are in excellent agreement. Figures 3 & 4 also show two hypothetical scenarios "no bombs" and "no fossil". The "no bombs" scenario shows how the decrease would have continued without nuclear atmospheric weapons testing, while "no fossils" show the situation without fossil fuel emissions.

Figure 5 shows the change in $\delta^{13}\text{C}$, with a standard deviation of 0.05‰, with the reduction being caused by Suess dilution (since fossil fuel emissions contains a lower level of ^{13}C) and by re-emission of CO_2 from the reservoir. This shape is also accurately tracked by the model.

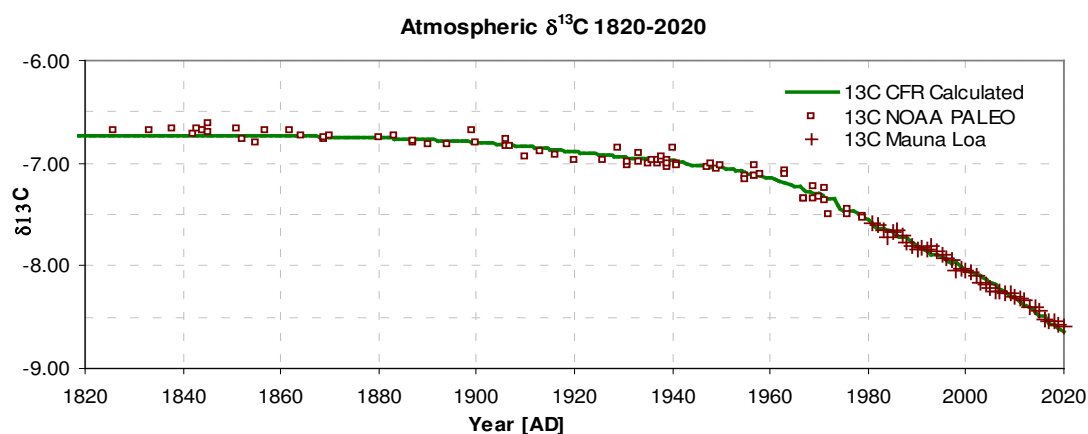


Figure 5. Atmospheric $\delta^{13}\text{C}$ 1820-2020. Model calculated values: solid green, Observed NOAA Paleo [D4]: squares, Mauna Loa [D2]: crosses, $\sigma_{1820-2020}=0.05\%$.

Table 1. Solved 7 Parameter Values.

Parameter	Sym.	Value	err.	Notes
Removal time (years)	α_t	14.87	1.7	Compares reasonably with Revelle & Suess (1957) of approximately 10 yr, and Arnold (1957) of 10-20 yr.
Relative Reservoir Size	RCO2	6.16	1.4	IPCC Ed., (2014) of 4250 GtC. $4250/588 = 7.2$.
CO2ff Uptake	Direct \otimes	0.56	0.11	See Discussion
Atomic Bomb Yield: $^{14}\text{C}/\text{MT}$	Yb	1.60	0.1	In mills. See Footnote
Pre-industrial ^{14}C ‰	$\Delta^{14}\text{C}$ nit	-3.1	10	Broad agreement with Intcal20[D6] for 1820 of 0.7‰. Max level between 1820-2020 is 800‰.
Pre-industrial ^{13}C ‰	$\otimes^{13}\text{C}$ nit	-6.7	0.2	Excellent agreement with Rubino (2013) 1820 of $\otimes^{13}\text{C} = 6.7$ ‰.
Fossil fuel ^{13}C ‰	$\otimes^{13}\text{C}_{\text{ff}}$	-20.4	4	Slightly low as compared to figures reported by Stuiver & Polach (1977) for coal of $\otimes^{13}\text{C} = -23$ ‰.

Nuclear Bomb Yield: The value returned is 1.6 ± 0.1 mills of ^{14}C per MT, with a total bomb yield of 440MT. For comparison, we convert the figures to estimates of the number of ^{14}C atoms per MT bomb yield using formulae derived from those of Svetlik (2010) and Strensom (2011). The number of carbon atoms in the atmosphere in 1950 with the CO_2 mixing level of 312.8 ppm corresponding to $A_{\text{CO}_2} = 664.43$ GtC, where the molecular weight of naturally abundant carbon, $\text{MC} = 12.01$, and Avogadro's number $N_A = 6.022 \times 10^{23}$, was

$$\text{NC} = A_{\text{CO}_2} \times N_A / \text{MC}$$

The $^{14}\text{C}/\text{C}$ ratio $R^{14}\text{C}$ can be obtained from the specific activity $\alpha = 0.226$ Bq per gram, ^{14}C half life $T_{1/2} = 5730$ years $= 1.807 \times 10^{11}$ s, molar weight of ^{14}C is $\text{MC}_{14} = 14$, and $\ln(2)$ as

$$R^{14}\text{C} = \alpha T_{1/2} \text{MC}_{14} / (N_A \times \ln(2))$$

The number of ^{14}C atoms $N^{14}\text{C}$ created is given by the product of the two expressions giving

$$N^{14}\text{C} = \text{NC} \times R^{14}\text{C} = (A_{\text{CO}_2} / \text{MC}) \times (\alpha T_{1/2} \text{MC}_{14} / \ln(2)) = 4.6 \times 10^{28}$$

Hence the number of ^{14}C atoms per MT of bomb yield is $0.0016 \times 4.6 \times 10^{28} = 7.4 \times 10^{25}$, comparing favourably with reported values by Hesshaimer et al. (1994) of 1 to 2×10^{26} atoms per MT. The total bomb yield of 440MT gives a figure of 3.23×10^{28} which compares with 6.1×10^{28} by Naegler & Levin (2006). The discrepancy may be due to ^{14}C which is stored but does not mix in the biosphere.

The amount of ^{14}C , also known as activity concentration, (as opposed to $\Delta^{14}\text{C}$), in the reservoir and atmosphere is shown in Figure 6. Their total (blue) represents the amount of ^{14}C in the system, the sudden step increase can be seen around 1960 due to atmospheric nuclear weapons testing. The atmospheric activity concentration shows the bomb pulse decaying to a minimum around 2000 but then rising slightly again, which has been experimentally reported by Svetlik (2010). The model shows the increase can be attributed to $^{14}\text{CO}_2$ re-emerging from the mixing reservoir, at the same time causing a slight drop in reservoir level.

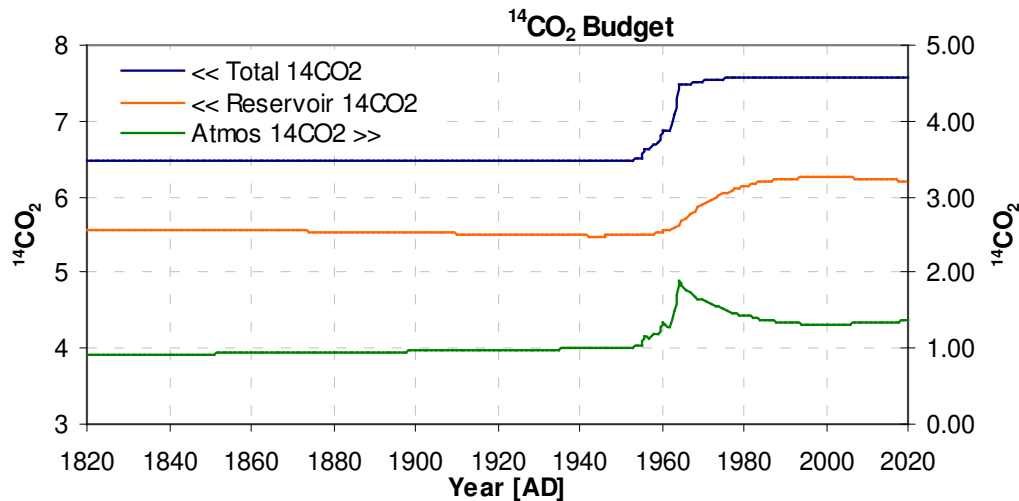


Figure 6. $^{14}\text{CO}_2$ Budget. Model derived absolute $^{14}\text{CO}_2$ (also known as activity concentration) for the reservoir (orange), the atmosphere (green), and their total (blue) in units relative to the $^{14}\text{CO}_2$ content of the atmosphere in 1950. The total, being the sum of reservoir plus atmosphere, shows the near step function in $^{14}\text{CO}_2$ created by nuclear atmospheric weapons testing. After the initial fall of atmospheric content, the small rise since 2000 is confirmed by the results of Svetlik [23] (see text).

4.1. Parameter Values

The solution of all seven parameter values, is listed in Table 1 along with their estimated error, which was derived by varying each parameter up and down, while holding the other parameter values constant, until the overall geometric mean standard deviation, σ , approximately doubled. The error figure was the mean of the two variations. For all the parameters except fossil-fuel direct uptake, the variation by the error figure causes an insignificant change in the flux figures, however in the case of fossil-fuel direct uptake the change in non-fossil input is from -10GtC to 83GtC , implying an uncertainty in non-fossil input from -3.5% sink to 29% source.

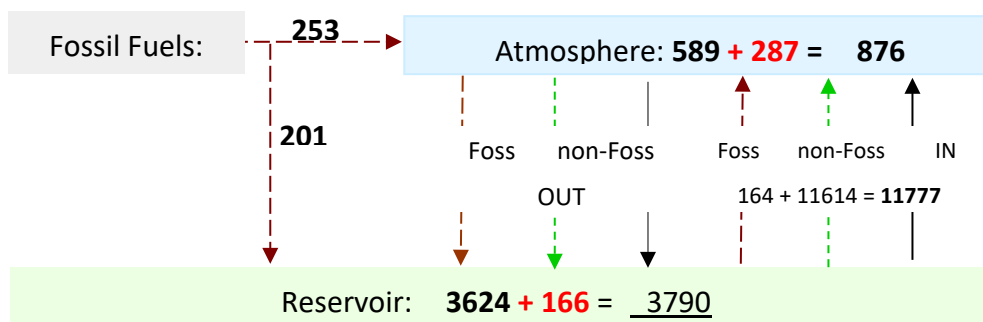


Figure 7. Atmospheric CO_2 levels and cumulative flux 1750 to 2020. (GtC) The figures in red represent the increase over the period, underscore indicates 2020 values. The concentration of CO_2 from fossil fuel emissions (CO_2ff) is higher in the atmosphere than in the reservoir, therefore the atmospheric flux OUT contains more CO_2ff than the flux IN, removing fossil fuel emissions from the atmosphere. Atmospheric $\text{CO}_2\text{ff} = 253 - 295 + 164 = 121$ (without rounding) corresponding to 13.9% of the atmosphere in 2020 (See Table 2, rows 3 / 9).

The study reports that, over the past 270 years, 27% of CO_2ff remains in the atmosphere corresponding to 13.9% of the atmospheric CO_2 content, and 88% of atmospheric growth is caused by CO_2ff (see Table 2). It is found that 44% of CO_2ff is directly absorbed into terrestrial biosphere and ocean with the remainder i.e. 56%, becoming mixed into the atmosphere. A small amount,

around 12% of atmospheric growth originates from natural sources although this figure had the largest uncertainty. See Discussion.

4.2. Flux and Cumulative Flux Output

Table 2 lists cumulative CO₂ flows and storage from 1750 to 2020, and 1960 to 2020, while fig. 7 shows the flux diagrammatically.

Table 2. Cumulative CO₂ Flow and Storage.

Duration	1750-2020 GtC	%	1960 -2020 GtC	%
CO₂ff Delivered				
delivered to Atmos. (β)	253	56	207	46
delivered to Rsvr. (1- β)	201	44	165	36
Total	454	100	372	82
CO₂ff by Destination				
In Atmos	121	27	100	26
In Rsvr	332	73	272	71
Total	454	100	382	100
Atmospheric Growth				
due to CO ₂ ff	253	88	207	102
due to non-Foss*	35	12	-3	-1
Total	287	100	204	100
Reservoir Growth				
due to CO ₂ ff	332		272	
due to non-Foss*	-166		-103	
Total	166		164	
Atmospheric Outflow				
CO ₂ ff	295		248	
non-Foss	11447		2798	
Total	11742		3045	
Reservoir Outflow				
CO ₂ ff	164		141	
non-Foss	11614		2902	
Total	11777		3042	
CO₂ff rel. to atmos CO₂ 2020†	121/876	14	100/876	11.5
CO₂ff induced growth/Co₂ff (AF)	253/454	55	56	
Average Annual Flux from Reservoir	43.7		50.8	
Average Annual Flux to Reservoir	43.5		50.9	

+ Relative to CO₂ff supplied; * Non-Foss means "not due to anthropogenic fossil fuel CO₂ emissions". † The CO₂ atmospheric mixing ratio in 2020 = 412 ppm, 876 GtC, in1750 = 277ppm, 589GtC. These values take into account the backflow of fossil fuel CO₂ from the reservoir to the atmosphere. Year Intervals are chosen to align with GCB from Friedlingstein (2021) Table 8. The flux / cumulative flux tables did not form part of the optimisation loop. Note that some of the figures are not model dependant, (e.g. CO₂ff Total, Atmospheric Growth Total) but are based upon subtractions of input data. See [3].Table 8.

4.3. Correlation of Inflow and Temperature

Figure 8 shows the absolute inflow (taken from the absolute model using the same 7 optimised parameters) and global temperature (D7) plotted on suitable vertical scales. The correlation coefficient is 0.94. Although correlation does not by itself imply causation, it is difficult to conceive of a mechanism whereby a global change in temperature could be caused by the rate of CO₂ inflow. The obvious temperature dependents mechanisms for CO₂ gas release in the ocean is the decrease of

solubility with temperature, while on land there is a balance between productivity, respiration and decay (Melillo et al. 2011). This evidence suggests that when global temperature increases, CO₂ absolute inflow also increases although it could be conceivable that both share a common cause. The absolute global inflow should not be confused with net figures which show a net uptake of anthropogenic CO₂.

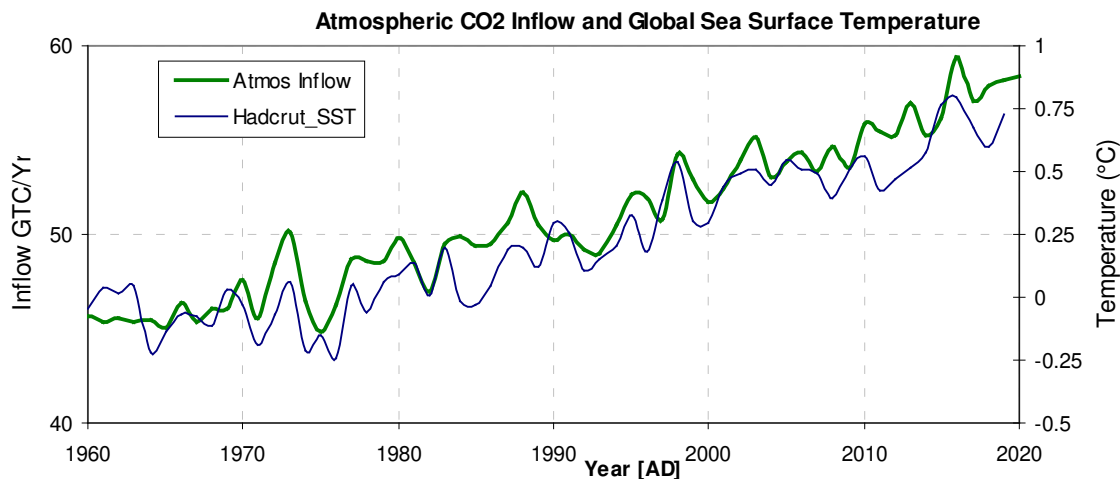


Figure 8. CO₂ inflow (green) and observed global sea-surface temperature (blue) indicating a high degree of correlation of 0.94.

5. Discussion

This section discusses the differences between this work and that of other authors. Some authors (e.g. Levin et al. 2010) have found it necessary to propose additional industrial pollution figures for ¹⁴C in order to close the ¹⁴C budget. This paper has no such requirement, yet accurately reproduces the ¹⁴C curve. A recently published work (Graven et al. 2020) used a model originally produced by M. Heimann and R. Keeling and rewritten for Matlab, to give results for a "no bombs" and "no fossil" scenarios, in a similar way to those shown in figure 5 of this paper. The results shown by Graven are almost identical to those shown here further vindicating the model described and its approach. Recent work by Svetlik (2010) showed measurements of the ¹⁴C activity concentration. This model produces an output of activity concentration which is very similar to that in Svetlik's work showing that the calculations regarding ¹⁴C are in broad agreement.

5.1. Isotopic Behaviour

It is a widely held view that the various isotopes of carbon in their molecular form of CO₂ behave differently when the exchange flux interacts with sea-water, bypassing carbonate chemistry (Revelle). This was first suggested by Siegenthaler and Oeschger (1987) and has been repeated many times since. It is claimed to lead to a factor of ten difference in isotopic behaviour of ¹³C and ¹⁴C as compared to ¹²C, thus preventing a straightforward analysis of the ¹⁴C bomb pulse (e.g. Harvey 2000). The argument is refuted here. It suggests isotope separation occurs naturally on a global scale. This is unlikely since, from a thermodynamic point of view, the isotopic mixture has a lower Gibbs free energy and lower entropy, requiring an expenditure of energy to achieve separation of its constituents (Seader & Henley 2005). We present here a further argument showing why we believe the claimed bypass effect does not occur in practice. Given the carbon concentration C and the isotopic ratio R the flux F_{14C} can be written as

$$F_{14C} = d(CR)/dt = R \cdot dC/dt + C \cdot dR/dt$$

The term, $R \cdot dC/dt$, describes the bulk flow of carbon without isotopic variation and hence suffers from carbonate chemistry while $C \cdot dR/dt$ represents the isotopic flow which it is claimed bypasses

seawater carbonate chemistry. We can better estimate the magnitude of the contribution of variations of either term, by dividing both sides by CR giving

$$\frac{A}{d(CR)/CR} = \frac{B}{dC/C + dR/R}$$

A comparison of the local values of the relative sizes of dC/C and dR/R indicates which term dominates. Fortunately one can obtain approximate estimates of these ratios in a variety of situations, over sea and land from a number of papers (e.g. Bishcof 1960, Dai et al. 2009, Faassen et al, 2022, Leinweber et al., 2009, Olsen et al. 2004, Palonen et al. 2018, Takahashi et al. 2002). It is essential to use local estimates rather than global nett figures, because nett figures would average out differences in isotopic content. The local variation of dC/C was estimated from the above references as of the order of ≈ 6 ppm/400ppm (≈ 0.015) per hour, with variation in dR/R for ^{14}C estimated as around $\approx 8\%$ (≈ 0.008) per hour and for ^{13}C $\approx 0.2 \%$ (≈ 0.0002) per hour. Hence $|A|$ amply dominates $|B|$. Therefore, it is irrelevant whether or not B has an ability to bypass carbonate chemistry (Revelle factor) as claimed by many, since A is the dominant effect. Regarding the A term how does it respond to different isotopes of carbon? According to (Zeebe and Wolf 2001: Section 2.5 Page 119) referring to three isotopic forms ^{12}C , ^{13}C and ^{14}C isotopic components "There are no direct reactions between each of these compartments... Thus there are three independent systems with respect to carbon isotopes." Furthermore there is only one common subsidiary chemical process, i.e. "chemical coupling of both systems brought about by the chemical reactions of the carbon compounds with "H+ and OH-". This is assumed here to be a relatively weak effect. Therefore in this study we consider the isotopic behaviour to be equal, although we accept there could be a small differences due to fractionation. The accuracy of the results for $\Delta^{14}\text{C}$ and $\delta^{13}\text{C}$ shown in Figures 3-5 results amply vindicates these assumptions, despite the widely held belief to the contrary. Furthermore, the values of the 7 parameters in Table 1 all have reasonable values, which seem extremely unlikely by chance. Therefore, regarding global absorption of atmospheric isotopic CO_2 by seawater, the argument is rejected that there is significant bypass of the Revelle factor.

5.2. Exchange Flow

As the earth daily rotates and annually orbits the sun, the terrestrial /oceanic reservoirs cyclically sucks in and blows out CO_2 . These are the exchange fluxes. In the model, the effective exchange flow is found to be around 50 GtC, considerably smaller than the IPCC figure of exchange flow at around 210 GtC. Consequently the exchange washout Residence Time (RT) in 1960 was around $C/Fe = 689/46 \sim 15$ years. Thus the residence time RT now aligns with the exponential decay of the atomic weapons pulse, without requiring the usual, but unlikely, hypothesis of unequal behaviour of isotopes. The difference in exchange flow arises because the model determines "effective values" which reflects the global average behaviour of molecular transfer, bearing in mind the mixing properties and cycle time lag (Oeschger 1975). Consider an analogy. Two isolated islands are separated by the services of a large passenger ferry. You may think the average residence time of a person on each island is given by the number of island inhabitants divided by the ferry flow. But the true average can be much less than this. How? Because the passenger ferry may carry much the same passengers back and forth, while many of the rural residents never take the ferry. Therefore the residence time is much longer because the "effective" washout flux is smaller. Similarly if the same exchange flow arises from decaying leaves and plant litter being cycled each year, the effective exchange flow is reduced, changing the residence time from around 4 years to 15.

5.3. Airborne Fraction

The Airborne Fraction, (AF) is said to be the ratio of " CO_2 remaining in the atmosphere" divided by "the anthropogenic CO_2 supplied" (Broeker 1975). It has been suggested that the reason for its constancy is related to the solution of an ordinary differential equation as applied to atmospheric CO_2 flux (Cawley 2011). According to this view, if the time constant for the exponential rate of rise of CO_2 matches the time constant for the rate of depletion of CO_2 then the Airborne Fraction

would be 0.5. However this paper suggests that the origin is quite different and is related to the direct uptake of CO₂ before the remainder is mixed into the atmosphere (Figure 1).

5.4. Direct Uptake

The presence of a direct uptake mechanism (as shown in Figure 1) significantly improves the model's accuracy, reducing the overall standard deviation by approximately 30%. Recent studies of daytime releases of ¹⁴CO₂ in the vicinity of nuclear power plants have reported significant ¹⁴CO₂ uptake (Naegler & Levin 2006) while a study of urban grasses near a major highway reported plants stored up to 13% of fossil-fuel carbon (Lichtfouse et al, 2005; Ota et al 2016). According to Kuderer et al (2018), "*The 14C signals from such point sources are well detectable in plant samples*". Therefore it seems reasonable to propose the existence of a direct uptake mechanism for CO₂ before it becomes mixed in the atmosphere. The effect of the direct uptake mechanism is to more rapidly transfer part of the rising CO₂ emissions to the reservoir, hence slightly changing the shape of the ¹⁴C and ¹³C curves.

5.5. 14 C Bomb Pulse

Regarding the shape of the bomb pulse, it would be expected that, if there is a constant level of washout exchange flux, its shape would be a reducing exponential converging back to its original background value. However simple inspection reveals this not to be the case. See Figure 4. This shape departs from an exponential decay because of three main reasons; a) incoming fossil fuel (free of ¹⁴C) is diluting the atmosphere, this being called "Suess Dilution" (Suess 1955), b) some of that incoming fossil fuel is also being washed out by the exchange flow and c) some of the incoming exchange flow has a higher level of ¹⁴C, because bomb ¹⁴C having accumulated in the oceans is now being re-emitted back to the atmosphere. If (a) was the sole cause of the deviation of the bomb curve shape from a pure exponential decay, the curve would be well below $\Delta^{14}\text{C}=0$, bearing in mind that the atmospheric growth of 30% is attributed to fossil fuel emissions containing no ¹⁴C. The effect of washout of fossil fuel emissions (b) raises the curve; this was noticed many years ago and termed by Stuiver and Quay (1981) the "attenuation factor". However the raise is still not quite sufficient to make a perfect match. Finally effect (c) raises the tail slightly further improving the fit to the current level shown in Figure 4.

Keeping track of all of these factors in a "back of the envelope" calculation is complex. The absolute flow model described calculates at each iteration ¹³C and ¹⁴C in reservoir and atmosphere (see Implementation section). It does not need to explicitly consider Suess dilution, the Stuiver attenuation factor, flow-back or the airborne factor as these emerge implicitly from the calculation.

5.6. Amount "Remaining" in the Atmosphere

The ambiguous meaning of "remaining" has led to some confusion between different authors; the situation is clarified here by extending the above island analogy further. Suppose one of the above islands, island A has an annual supply of people arriving via its Airport, increasing its population. The ferry continues to carry exactly the same number of people back and forth between island A and island B. The population of the island A increases, yet over time the ferry has carried many of the airport arrivals to island B, and has brought inhabitants back from B to A in their place. A census would report that the number of people on island A who flew in, is less than its population growth because some are living on island B. However others would say that airport arrivals caused 100% of the growth of A since without airport arrivals their population would not have grown. This illustrates the discrepancy. IPCC state "*The combustion of fossil fuels and land-use change for the period 1750–2019 resulted in the release of 700 ± 75 PgC (likely range, $1 \text{ PgC} = 10^{15} \text{ g of carbon}$) to the atmosphere, of which about $41\% \pm 11\%$ remains in the atmosphere today (high confidence)*" (IPCC 2023 p80). However the amount "remaining" of CO₂ has been found by Skrabale to be 23% and in this paper to be 27%. The apparent discrepancy arises because a) a significant part of CO₂ causing the growth has been washed out and almost exactly replaced by the exchange flow, and b) because the IPCC figure includes an allowance for Land Use Change (LUC) which cannot be accounted for by the isotopic

method because of its unknown isotopic signature (although LUC has significantly reduced in recent years). The alternative measure of molecular CO₂ remaining relative to atmospheric CO₂ content was provided by Skrable (12%), Stallinga (<10%), this paper (14%) providing reasonable agreement between the three authors.

6. Conclusions

A two box CO₂ absolute flow model is described which

- accurately predicts the values of $\delta^{14}\text{C}$ and $\delta^{13}\text{C}$ over 200 years.
- revises the view of the airborne fraction, proposing that it reflects the relative amount of CO₂ff that is absorbed directly into the terrestrial/oceanic reservoir,
- does not use or require a consideration of carbonate seawater chemistry (Revelle),
- shows there is no practical significant difference in behaviour of different isotopes apart from fractionation
- explains how exponential decay time of the bomb pulse does, after all, relate to the residence time,
- resolves the conflicting calculations of how much CO₂ff "remains" in the atmosphere.

The method produces annual estimates of both nett inflow and the individual exchange flows, making it possible to calculate the molecular CO₂ff remaining and also to provide the amount of atmospheric growth due to CO₂ff. Thus the model leads to new estimates for the period 1750 to 2020 of the partitioning of anthropogenic CO₂ emissions, with 88% of growth being attributable to CO₂ fossil fuel emissions, and 12% being due to net "natural" emissions from the terrestrial and oceanic source, including land use change. Relative to total CO₂ff of 454 GtC, 253 GtC or 55% was accountable for the growth of the atmosphere. However, at the molecular level, because of the washout caused by exchange flow, only 27% of fossil fuel emissions remain airborne, which corresponds to 14% of the entire CO₂ atmosphere. The model uniquely provides both figures thus helping to resolve any confusion regarding the meaning and effects of fossil fuel CO₂ emissions.

Acknowledgments: I would like to thank my colleague Dr. Andrew Layfield (Engineering and Environmental Studies), City University, Hong Kong, for his detailed comments and proofreading. The author would like to thank and acknowledge all the data providers indicated in "Data References", without whom this work could never have been carried out. This research was self-funded and received no external funding. The author declares no conflict of interest. The author would like to thank the publisher for reducing the APC which was funded by the publisher.

References

1. Arnold, J.R., 1957. The Distribution of Carbon-14 in Nature. *Tellus* 9, 28–32. <https://doi.org/10.1111/j.2153-3490.1957.tb01850.x>
2. Ballantyne, A.P., Alden, C.B., Miller, J.B., Tans, P.P., White, J.W.C., 2012. Increase in observed net carbon dioxide uptake by land and oceans during the past 50 years. *Nature* 488, 70–72. <https://doi.org/10.1038/nature11299>
3. Bischof, W., 1960. Periodical Variations of the Atmospheric CO₂ -content in Scandinavia. *Tellus* 12, 216–226. <https://doi.org/10.1111/j.2153-3490.1960.tb01303.x>
4. Broecker, W.S., 1975. Climatic Change: Are We on the Brink of a Pronounced Global Warming? *Science* 189, 460–463. <https://doi.org/10.1126/science.189.4201.460>
5. Cawley, G.C., 2011. On the Atmospheric Residence Time of Anthropogenically Sourced Carbon Dioxide. *Energy Fuels* 25, 5503–5513. <https://doi.org/10.1021/ef200914u>
6. Dai, M., Lu, Z., Zhai, W., Chen, B., Cao, Z., Zhou, K., Cai, W.-J., Chenc, C.-T.A., 2009. Diurnal variations of surface seawater pCO₂ in contrasting coastal environments. *Limnol. Oceanogr.* 54, 735–745. <https://doi.org/10.4319/lo.2009.54.3.0735>
7. Faassen, K.A.P., Nguyen, L.N.T., Broekema, E.R., Kers, B.A.M., Mammarella, I., Vesala, T., Pickers, P.A., Manning, A.C., Vilà-Guerau De Arellano, J., Meijer, H.A.J., Peters, W., Lujckx, I.T., 2022. Diurnal variability of atmospheric O₂, CO₂ and their exchange ratio above a boreal forest in southern Finland (preprint).

- Gases/Field Measurements / Troposphere / Physics (physical properties and processes).
<https://doi.org/10.5194/acp-2022-504>
8. Friedlingstein, P., Jones, M.W., O'Sullivan, M., Andrew, R.M., Bakker, D.C.E., Hauck, J., Le Quéré, C., Peters, G.P., Peters, W., Pongratz, J., Sitch, S., Canadell, J.G., Ciais, P., Jackson, R.B., Alin, S.R., Anthoni, P., Bates, N.R., Becker, M., Bellouin, N., Bopp, L., Chau, T.T.T., Chevallier, F., Chini, L.P., Cronin, M., Currie, K.I., Decharme, B., Djeutchouang, L.M., Dou, X., Evans, W., Feely, R.A., Feng, L., Gasser, T., Gilfillan, D., Gkritzalis, T., Grassi, G., Gregor, L., Gruber, N., Gürses, Ö., Harris, I., Houghton, R.A., Hurtt, G.C., Iida, Y., Ilyina, T., Luijkx, I.T., Jain, A., Jones, S.D., Kato, E., Kennedy, D., Klein Goldewijk, K., Knauer, J., Korsbakken, J.I., Körtzinger, A., Landschützer, P., Lauvset, S.K., Lefèvre, N., Lienert, S., Liu, J., Marland, G., McGuire, P.C., Melton, J.R., Munro, D.R., Nabel, J.E.M.S., Nakaoka, S.-I., Niwa, Y., Ono, T., Pierrot, D., Poulter, B., Rehder, G., Resplandy, L., Robertson, E., Rödenbeck, C., Rosan, T.M., Schwinger, J., Schwingshackl, C., Séférian, R., Sutton, A.J., Sweeney, C., Tanhua, T., Tans, P.P., Tian, H., Tilbrook, B., Tubiello, F., Van Der Werf, G.R., Vuichard, N., Wada, C., Wanninkhof, R., Watson, A.J., Willis, D., Wiltshire, A.J., Yuan, W., Yue, C., Yue, X., Zaehle, S., Zeng, J., 2022. Global Carbon Budget 2021. *Earth Syst. Sci. Data* 14, 1917–2005. <https://doi.org/10.5194/essd-14-1917-2022>
 9. Graven, H., Keeling, R.F., Rogelj, J., 2020. Changes to Carbon Isotopes in Atmospheric CO₂ Over the Industrial Era and Into the Future. *Global Biogeochemical Cycles* 34, e2019GB006170. <https://doi.org/10.1029/2019GB006170>
 10. Harvey, L.D.D., 2000. *Global warming: the hard science*, 1. publ. ed, Pearson education. Prentice Hall, Harlow Munich. Routledge, (2018) ISBN 0582-38167-3
 11. Hesshaimer, V., Heimann, M., Levin, I., 1994. Radiocarbon evidence for a smaller oceanic carbon dioxide sink than previously believed. *Nature* 370, 201–203. <https://doi.org/10.1038/370201a0>
 12. Houghton, J.T., Intergovernmental Panel on Climate Change (Eds.), 1996. *Climate change 1995: the science of climate change*. Cambridge University Press, Cambridge ; New York.
 13. Hua, Q., Turnbull, J.C., Santos, G.M., Rakowski, A.Z., Ancapichún, S., De Pol-Holz, R., Hammer, S., Lehman, S.J., Levin, I., Miller, J.B., Palmer, J.G., Turney, C.S.M., 2022. ATMOSPHERIC RADIOCARBON FOR THE PERIOD 1950–2019. *Radiocarbon* 64, 723–745. <https://doi.org/10.1017/RDC.2021.95>
 14. Intergovernmental Panel On Climate Change (Ed.), 2014. *Carbon and Other Biogeochemical Cycles*, in: *Climate Change 2013 – The Physical Science Basis*. Cambridge University Press, pp. 465–570. <https://doi.org/10.1017/CBO9781107415324.015>
 15. Intergovernmental Panel On Climate Change, 2023. *Climate Change 2021 – The Physical Science Basis: Working Group I Contribution to the Sixth Assessment Report of the Intergovernmental Panel on Climate Change*, 1st ed. Cambridge University Press. <https://doi.org/10.1017/9781009157896>
 16. Joos, F., 1994. Imbalance in the budget. *Nature* 370, 181–182. <https://doi.org/10.1038/370181a0>
 17. Joos, F., Bruno, M., Fink, R., Siegenthaler, U., Stocker, T.F., Le Quéré, C., Sarmiento, J.L., 1996. An efficient and accurate representation of complex oceanic and biospheric models of anthropogenic carbon uptake. *Tellus B: Chemical and Physical Meteorology* 48, 397. <https://doi.org/10.3402/tellusb.v48i3.15921>
 18. Kutschera, W., 2013. Applications of accelerator mass spectrometry. *International Journal of Mass Spectrometry* 349–350, 203–218. <https://doi.org/10.1016/j.ijms.2013.05.023>
 19. Leinweber, A., Gruber, N., Frenzel, H., Friederich, G. E., and Chavez, F. P., 2009, Diurnal carbon cycling in the surface ocean and lower atmosphere of Santa Monica Bay, California, *Geophys. Res. Lett.*, 36,L08601, doi:10.1029/2008GL037018.
 20. Levin, I., Naegler, T., Kromer, B., Diehl, M., Francey, R.J., Gomez-Pelaez, A.J., Steele, L.P., Wagenbach, D., Weller, R., Worthy, D.E., 2010. Observations and modelling of the global distribution and long-term trend of atmospheric ¹⁴CO₂. *Tellus B: Chemical and Physical Meteorology* 62, 26. <https://doi.org/10.1111/j.1600-0889.2009.00446.x>
 21. Lichtfouse, E., Lichtfouse, M., Kashgarian, M., Bol, R., 2005. ¹⁴C of grasses as an indicator of fossil fuel CO₂ pollution. *Environ Chem Lett* 3, 78–81. <https://doi.org/10.1007/s10311-005-0100-4>
 22. Kuderer, Matthias, Samuel Hammer, and Ingeborg Levin. "The Influence of ¹⁴CO₂ Releases from Regional Nuclear Facilities at the Heidelberg ¹⁴CO₂ Sampling Site (1986–2014)." *Atmospheric Chemistry and Physics* 18, no. 11 (June 6, 2018): 7951–59. <https://doi.org/10.5194/acp-18-7951-2018>.
 23. Melillo, J.M., Butler, S., Johnson, J., Mohan, J., Steudler, P., Lux, H., Burrows, E., Bowles, F., Smith, R., Scott, L., Vario, C., Hill, T., Burton, A., Zhou, Y.-M., Tang, J., 2011. Soil warming, carbon–nitrogen interactions, and forest carbon budgets. *Proc. Natl. Acad. Sci. U.S.A.* 108, 9508–9512. <https://doi.org/10.1073/pnas.1018189108>
 24. Naegler, T., Levin, I., 2006. Closing the global radiocarbon budget 1945–2005. *J. Geophys. Res.* 111, D12311. <https://doi.org/10.1029/2005JD006758>
 25. Ota, M., Katata, G., Nagai, H., Terada, H., 2016. Impacts of C-uptake by plants on the spatial distribution

- of 14 C accumulated in vegetation around a nuclear facility—Application of a sophisticated land surface 14 C model to the Rokkasho reprocessing plant, Japan. *Journal of Environmental Radioactivity* 162–163, 189–204. <https://doi.org/10.1016/j.jenvrad.2016.05.032>
26. Oeschger, H., Siegenthaler, U., Schotterer, U., Gugelmann, A., 1975. A box diffusion model to study the carbon dioxide exchange in nature. *Tellus A: Dynamic Meteorology and Oceanography* 27, 168. <https://doi.org/10.3402/tellusa.v27i2.9900>
 27. Olsen, A., Omar, A. M., Stuart-Menteth, A. C., and Triñanes, J. A., 2004, Diurnal variations of surface ocean $p\text{CO}_2$ and sea-air CO_2 flux evaluated using remotely sensed data, *Geophys. Res. Lett.*, 31, L20304, doi:10.1029/2004GL020583.
 28. Palonen, V., Pumpanen, J., Kulmala, L., Levin, I., Heinonsalo, J., Vesala, T., 2018. Seasonal and Diurnal Variations in Atmospheric and Soil Air ^{14}C in a Boreal Scots Pine Forest. *Radiocarbon* 60, 283–297. <https://doi.org/10.1017/RDC.2017.95>
 29. Popper, Karl. 1934. *Logik der Forschung* [The Logic of Scientific Discovery] (2nd ed.). Reprint 1962. *La lógica de la investigación científica*. Tecnos, Madrid. Reprint 1992. London: Routledge. pp. 121–132. (1992) ISBN 978-84-309-0711-3.
 30. Revelle, R., Suess, H.E., 1957. Carbon Dioxide Exchange Between Atmosphere and Ocean and the Question of an Increase of Atmospheric CO_2 during the Past Decades. *Tellus* 9, 18–27. <https://doi.org/10.3402/tellusa.v9i1.9075>
 31. Rubino, M., Etheridge, D.M., Trudinger, C.M., Allison, C.E., Battle, M.O., Langenfelds, R.L., Steele, L.P., Curran, M., Bender, M., White, J.W.C., Jenk, T.M., Blunier, T., Francey, R.J., 2013. A revised 1000 year atmospheric $\delta^{13}\text{C}-\text{CO}_2$ record from Law Dome and South Pole, Antarctica: 1000 YEARS OF ATMOSPHERIC $\delta^{13}\text{C}-\text{CO}_2$. *J. Geophys. Res. Atmos.* 118, 8482–8499. <https://doi.org/10.1002/jgrd.50668>
 32. Seader, J.D., Henley, E.J., Roper, D.K., 2011. *Separation Process Principles with Applications using Process Simulators*, 3rd ed. ed. Wiley, Somerset. ISBN 1118139623
 33. Siegenthaler, U., Oeschger, H., 1987. Biospheric CO_2 emissions during the past 200 years reconstructed by deconvolution of ice core data. *Tellus B: Chemical and Physical Meteorology* 39, 140. <https://doi.org/10.3402/tellusb.v39i1-2.15331>
 34. Skrabble, K., Chabot, G., French, C., 2022. World Atmospheric CO_2 , Its ^{14}C Specific Activity, Non-fossil Component, Anthropogenic Fossil Component, and Emissions (1750–2018). *Health Physics* 122, 291–305. <https://doi.org/10.1097/HP.0000000000001485>
 35. Stallinga, P., 2023. Residence Time vs. Adjustment Time of Carbon Dioxide in the Atmosphere. *Entropy* 25, 384. <https://doi.org/10.3390/e25020384>
 36. Stenström, K, Skog, G, Georgiadou, E, Genberg, J & Mellström, A. 2011. A guide to radiocarbon units and calculations. LUNFD6(NFFR-3111)/1-17/(2011), Lund University, Nuclear Physics..
 37. Stuiver, M., Polach, H.A., 1977. Discussion Reporting of ^{14}C Data. *Radiocarbon* 19, 355–363. <https://doi.org/10.1017/S0033822200003672>
 38. Stuiver, M., Quay, P.D., 1981. Atmospheric ^{14}C changes resulting from fossil fuel CO_2 release and cosmic ray flux variability. *Earth and Planetary Science Letters* 53, 349–362. [https://doi.org/10.1016/0012-821X\(81\)90040-6](https://doi.org/10.1016/0012-821X(81)90040-6)
 39. Stuiver, M., Reimer, P.J., Bard, E., Beck, J.W., Burr, G.S., Hughen, K.A., Kromer, B., McCormac, G., Van Der Plicht, J., Spurk, M., 1998. INTCAL98 Radiocarbon Age Calibration, 24,000–0 cal BP. *Radiocarbon* 40, 1041–1083. <https://doi.org/10.1017/S0033822200019123>
 40. Suess, H.E., 1955. Radiocarbon Concentration in Modern Wood. *Science* 122, 415–417. <https://doi.org/10.1126/science.122.3166.415.b>
 41. Svetlik, I., Povinec, P.P., Molnár, M., Meinhardt, F., Michálek, V., Simon, J., Svingor, É., 2010. Estimation of Long-Term Trends in the Tropospheric ^{14}C Activity Concentration. *Radiocarbon* 52, 815–822. <https://doi.org/10.1017/S0033822200045835>
 42. Takahashi, H.A., Konohira, E., Hiyama, T., Minami, M., Nakamura, T., Yoshida, N., 2002. Diurnal variation of CO_2 concentration, $\Delta^{14}\text{C}$ and $\delta^{13}\text{C}$ in an urban forest: estimate of the anthropogenic and biogenic CO_2 contributions. *Tellus B: Chemical and Physical Meteorology* 54, 97. <https://doi.org/10.3402/tellusb.v54i2.16651>
 43. Tans, P.P., Berry, J.A., Keeling, R.F., 1993. Oceanic $^{13}\text{C}/^{12}\text{C}$ observations: A new window on ocean CO_2 uptake. *Global Biogeochemical Cycles* 7, 353–368. <https://doi.org/10.1029/93GB00053>
 44. Tans, P., 2022. Reminiscing On The Use And Abuse Of ^{14}C And ^{13}C In Atmospheric CO_2 . *Radiocarbon* 64, 747–760. <https://doi.org/10.1017/RDC.2022.7>
 45. Zeebe, Richard E., and Dieter Wolf-Gladrow. 2001. *CO_2 in Seawater: Equilibrium, Kinetics, Isotopes*. Gulf Professional Publishing, 2001. ISBN 9780444509468

Data References

1. Institute for Atmospheric and Climate Science (IAC), CO2 Mean Global AD0 to AD2014
ftp://data.iac.ethz.ch/CMIP6/input4MIPs/UoM/GHGConc/CMIP/yr/atmos/UoM-CMIP-1-1-0/GHGConc/gr3-GMNHSH/v20160701/mole_fraction_of_carbon_dioxide_in_air_input4MIPs_GHGConcentrations_CMIP_UoM-CMIP-1-1-0_gr3-GMNHSH_0000-2014.csv
2. NOAA GML. Accessed 04-March-2022. https://gml.noaa.gov/ccgg/trends/gl_data.html File: https://gml.noaa.gov/webdata/ccgg/trends/co2/co2_annmean_gl.txt
3. Global Carbon Budget: National_Carbon_Emissions_2021v0.4.xlsx Historical Budget, Global Fossil Emissions Visited 04 March 2022. Friedlingstein et al (2021),
4. World Data Service for Paleoclimatology, Boulder and NOAA Paleoclimatology Program, National Centers for Environmental Information (NCEI) <https://www1.ncdc.noaa.gov/pub/data/paleo/icecore/antarctica/law/law2018d13c-co2.txt>, <https://doi.org/10.25919/5bfe29ff807fb>
5. UNSCEAR: United Nations Scientific Committee on the Effects of Atomic Radiation 2000 Report To The General Assembly. Volume I: Sources. Annex C: Exposures To The Public From Man-Made Sources Of Radiation 207 Sources And Effects Of Ionizing Radiation. Table 4. Annual Fission And Fusion Yields.
6. Calib: INTCAL20/SGCAL20. Stuiver, M. et al, 2022 CALIB 8.2 [WWW program] at <http://calib.org>, accessed 2022-3-4 Rev 8.1.0 intcal20.14c, shcal20.14c
7. HADCRUT4, <https://www.metoffice.gov.uk/hadobs/>
8. hadcrut4 /data/current/time_series/ HadCRUT.4.6.0.0.monthly_ns_avg.txt, hadsst4/data/csv/ HadSST.4.0.0.0_monthly_GLOBE.csv

Disclaimer/Publisher's Note: The statements, opinions and data contained in all publications are solely those of the individual author(s) and contributor(s) and not of MDPI and/or the editor(s). MDPI and/or the editor(s) disclaim responsibility for any injury to people or property resulting from any ideas, methods, instructions or products referred to in the content.